IEEE Access
Multidisciplinary : Rapid Review : Open Access Journal

Received 27 June 2023, accepted 3 July 2023, date of publication 13 July 2023, date of current version 21 July 2023.

*Digital Object Identifier 10.1109/ACCESS.2023.3294973*

APPLIED RESEARCH

# High Power Microwave Signal Generation Based on Recursive Balanced Power Amplifier

**HAN LIM LEE[1], (Member, IEEE), SEUNG PYO PARK[2], AND MOON-QUE LEE[2], (Member, IEEE)**
[1]School of Electrical and Electronics Engineering, Chung-Ang University, Seoul 06974, South Korea
[2]School of Electrical and Computer Engineering, University of Seoul, Seoul 02504, South Korea

Corresponding author: Moon-Que Lee (mqlee@uos.ac.kr)

The work of Han Lim Lee was supported by the Institute for Information and Communications Technology Promotion (IITP) Grant funded by the Korea Government (MSIP), Development of W-Band Chirp Radar RFIC for Level Sensor, under Grant 2021-0-00151. The work of Moon-Que Lee was supported by the 2021 Research Fund of the University of Seoul.

**ABSTRACT** This paper presents a high-power microwave oscillator using a recursive balanced amplification technique. The proposed architecture is configured by a balanced power amplifier (BPA) with class-AB operation and two feedback networks. Each feedback circuit consists of a phase shifter and a high-Q bandpass filter (BPF). The BPA consists of an input hybrid coupler (IHC) and an output hybrid coupler (OHC) to divide and recombine signals amplified through two power amplifiers (PAs) connected in parallel. The outputs of the OHC and the inputs of the IHC are connected to form a positive feedback loop for oscillation. The signal from each output of the OHC continuously and alternately feedbacks to each input of the IHC, resulting in recursive amplifications for high power oscillation. The proposed high power oscillator was designed at 915 MHz with the measured output power of 38.62 dBm. The measured DC-to-RF conversion efficiency was 44.43%. Furthermore, the measured phase noises were −118.42 dBc/Hz and −124 dBc/Hz at 10 kHz and 100 kHz offsets, respectively.

**INDEX TERMS** Balanced power amplifier, high-power oscillator, microwave signal generation, recursive amplifier, regenerative oscillator.

## I. INTRODUCTION

The demand for wireless devices using wider bandwidth through higher frequency is continuously increasing with the evolution of high-speed communications. As a result, high efficiency and low complexity design approaches are considered as the fundamental requirement for high frequency wireless components. Among many different building blocks, microwave oscillators are the key component to build a successful wireless system including communications, radars, navigations, or sensors since they are used for various purposes in high frequencies [1], [2], [3], [4], [5], [6], [7]. For example, microwave oscillators can be used for high frequency synchronization, electromagnetic wave generation, and local signals in frequency converters. Despite there being many different applications requiring microwave signal generation, high power microwave generations are mostly focused in military or industrial applications. Typical high-power generation or amplification are based on travelling wave tube (TWT), magnetron, klystron, and solid-state structures [8], [9], [10], [11], [12], [13].

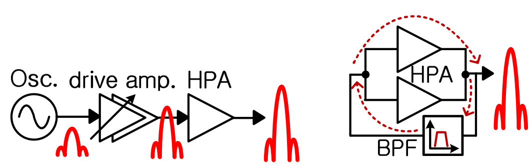


**FIGURE 1. High power microwave signal generation with (a) conventional cascade and (b) proposed RBPA configurations.**

Although the TWT, magnetron and klystron based architectures can generate several kW to MW output power, relatively larger bias voltage is required than the solid-state power amplifiers (PAs). To consider the applications where limited supply voltage level is used, solid-state power amplifier (SSPA) based architecture is rather focused in this paper.

The associate editor coordinating the review of this manuscript and approving it for publication was Tae Wook Kim.

The conventional SSPA based configuration to generate high power microwave signals consists of a source oscillator, multiple stage drive amplifiers and high power amplifier (HPA) as shown in Fig. 1 (a). One of the major challenges in high power microwave signal generation is the difficulty in achieving high efficiency due to the multiple drive amplifiers providing sufficient gain for HPA's maximum output power. To alleviate the efficiency burdens in both power consumption and system configuration, a recursive balanced power amplifier (RBPA) based microwave signal generation as shown in Fig. 1 (b) is proposed in this paper.

The fundamental configuration is a feedback amplifier based oscillator, where the inputs and outputs of the balanced power amplifier (BPA) are connected through phase-controllable feedback networks. The oscillation frequency is selected by a high-Q bandpass filer (BPF) and a phase shifter integrated within the loop to satisfy Barkhausen conditions for oscillation. By adopting the proposed structure, driver amplifiers to provide high gain to the HPA can be eliminated, resulting in an improved power consumption efficiency. To verify the proposed structure, the rest of this paper is organized by designing and analyzing required blocks, and the complete microwave signal generator in section II. Then, the proposed structure is implemented and verified by experiments in section III. Lastly, a conclusion is made in section IV.

## II. DESIGN AND ANAYSIS OF THE PROPOSED HIGH OUTPUT POWER MICROWAVE SIGNAL GENERATOR

The conventional high power microwave signal generation is usually configured by a low power oscillator and HPA cascaded with multistage drive amplifiers. However, the multistage high gain drive amplifiers usually degrade the overall DC-to-RF conversion efficiency and become the unwanted noise amplification source within a printed circuit board (PCB) due to its high gain. Instead of adopting the low power oscillation source with cascaded drive amplifiers, the proposed structure adopts a BPA with recursive feedback networks. Here, the balanced inputs and outputs are designed to form positive feedback loops. Fig. 2 (a) shows the proposed architecture configured by the BPA with class-AB operation and two feedback loops consisting of high-Q BPFs and phase shifters. Although Fig. 2 (a) includes isolators in the feedback loops, they can be optionally used to increase the reverse isolation for the BPA. The BPA consists of input hybrid coupler (IHC) and output hybrid coupler (OHC) to divide and recombine signals amplified through two PAs connected in parallel. The outputs of the OHC and the inputs of the IHC are connected to form a positive feedback loop to create oscillation. Here, the high-Q BPF and phase shifter determine the oscillation frequency. The signal from each output of the OHC continuously and alternately feedbacks to each input of the IHC, resulting in recursive amplification until the PA becomes saturated. It is noted that a coupling capacitor is used to sample an output signal to one of the two feedback loops, while the same node is also used for oscillator output port.

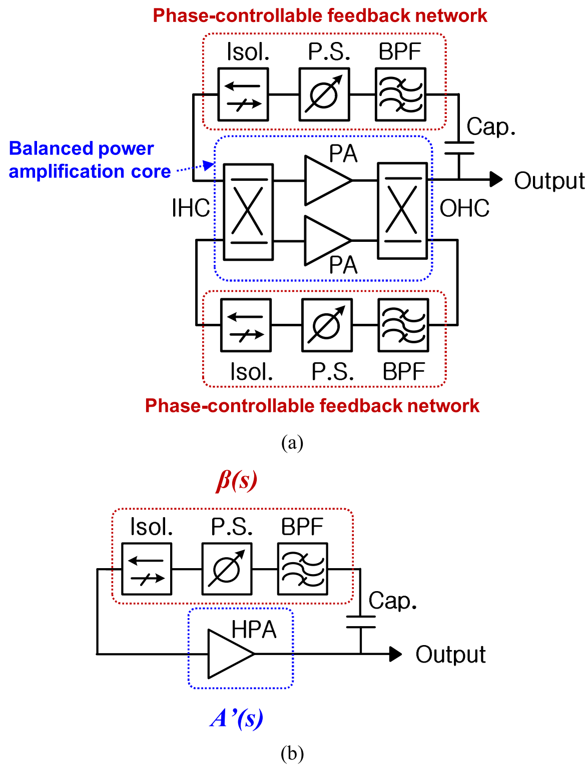


**FIGURE 2. Proposed architecture with (a) complete circuitry and (b) simplified circuitry.**

According to Fig. 2 (a), the open-loop gain characteristic of the BPA can be represented by $A(s)$ while the two identical feedback networks can be represented with a time-varying feedback factor, $\beta(s)$. Then, the oscillation can be initiated by the Barkhausen Criteria, $|A\beta| \geq 1$ and $\angle A\beta = 2\pi n$ (n = 0, 1, 2, ...). Unlike using a single PA, the BPA gain is slightly lower than the gain of single PA used in the balanced structure due to the insertion losses of IHC and OHC. Furthermore, division and recombination losses can occur though the IHC and OHC if amplitude and phase imbalances between each PA exist [14], [15], [16]. That is, the total gain of BPA depends on the gain of single PA, insertion loss and mismatch loss of the hybrid couplers. Then, the active open-loop gain can be equivalently represented by $A'(s)$ including the above-mentioned losses as shown in Fig. 2 (b). Here, the magnitude of $A'(s)$ is less than the magnitude of $A(s)$. To overcome the decrease in the gain of BPA and eliminate the use of extra drive amplifier as used in the conventional cascade structure, recursive structure can be applied to the conventional BPA. Fig. 3 (a) shows the conventional BPA, where the output port depends on the input port. For example, if the input 1 is used as the input port, the output comes out from the output 1 whereas the output 2 can be only used by the input 2. According to Fig. 3 (b), if one of the output ports of OHC is fed back to the other input port of IHC, the recursive signal can be re-amplified and outputted to the other output port. Here, the incoming signal phases must be maintained at the two input ports of IHC to generate the output power properly. If the recursive path can provide the proper phase delay,

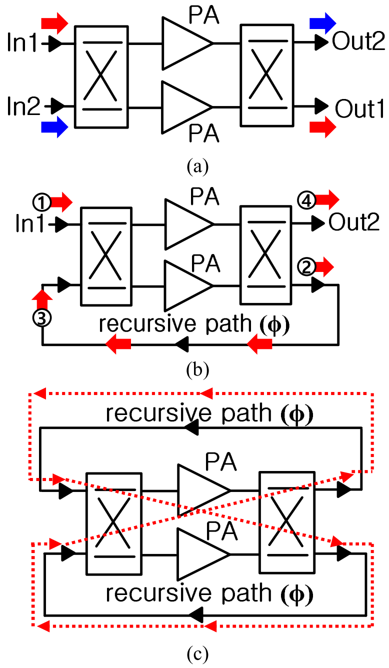


**FIGURE 3.** Input-to-output relationship by (a) conventional BPA, (b) RBPA and (c) RBPA-based oscillator.

the gain of BPA can be approximately doubled. Therefore, by combining both BPA and feedback network, the driverless RBPA can be used as the oscillator as shown in Fig. 3 (c).

The BPA is first designed by using two Laterally Diffused Metal Oxide Semiconductor (LDMOS) class-AB PAs and two branch-line couplers. Although GaN devices can be used for further increasing the output power with higher efficiency, reduction in cost is primarily considered in this paper. Thus, the PA is designed with a commercially available LDMOS RF power transistor, MW6S004NT1, from NXP semiconductors. The selected RF power MOSFET has a typical gain of 19 dB, drain efficiency of 33%, breakdown voltage of 68 V, and a typical output power of 36 dBm from 1 to 2000 MHz depending on the matching characteristics. Based on source and load pull simulations from 800 to 1000 MHz, the input and output impedances are determined at 915 MHz considering the maximum output power of 36 dBm as shown in Fig 4 (a) and (b). Then, a single stage class-AB PA is designed with the input and output matching networks including the gate and drain biasing networks as shown in Fig. 4 (c). For the class-AB operation, the drain voltage of 28 V and the gate voltage of 2.7 V are used. Also, the PA is designed with a Teflon substrate having a relative permittivity of 2.54 and a thickness of 0.5 mm. Fig. 4 (d) shows the simulated S-parameters of the designed PA, where the small signal gain and the 10-dB impedance bandwidth are about 20 dB and 100 MHz, respectively. Also, the simulated output 1-dB compression point (P1-dB) of 36 dBm is achieved at 915 MHz as shown in Fig. 4 (e). Next, to reduce the overall size of the BPA, commercially available low-loss LTCC branch-line couplers

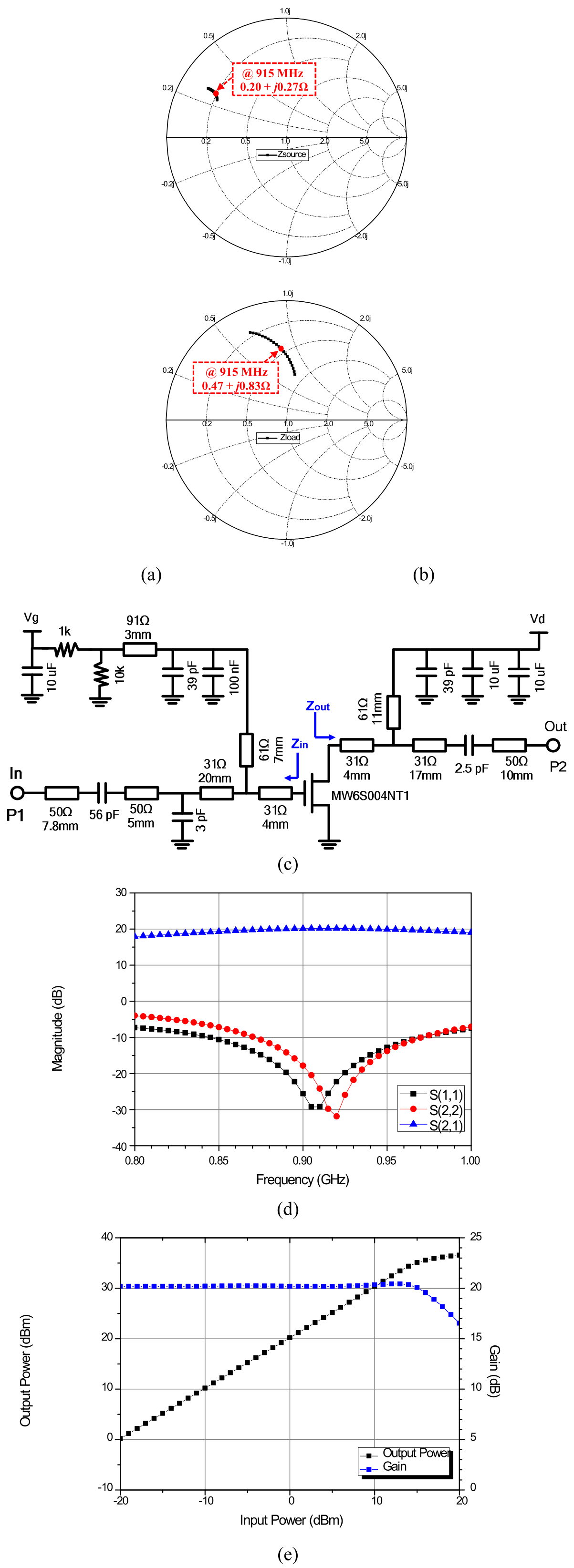


**FIGURE 4.** Single-stage class-AB PA with (a) -(b) simulated source and load impedances, (c) circuit schematic, (d) simulated S-parameters, and (e) simulated output power and gain.

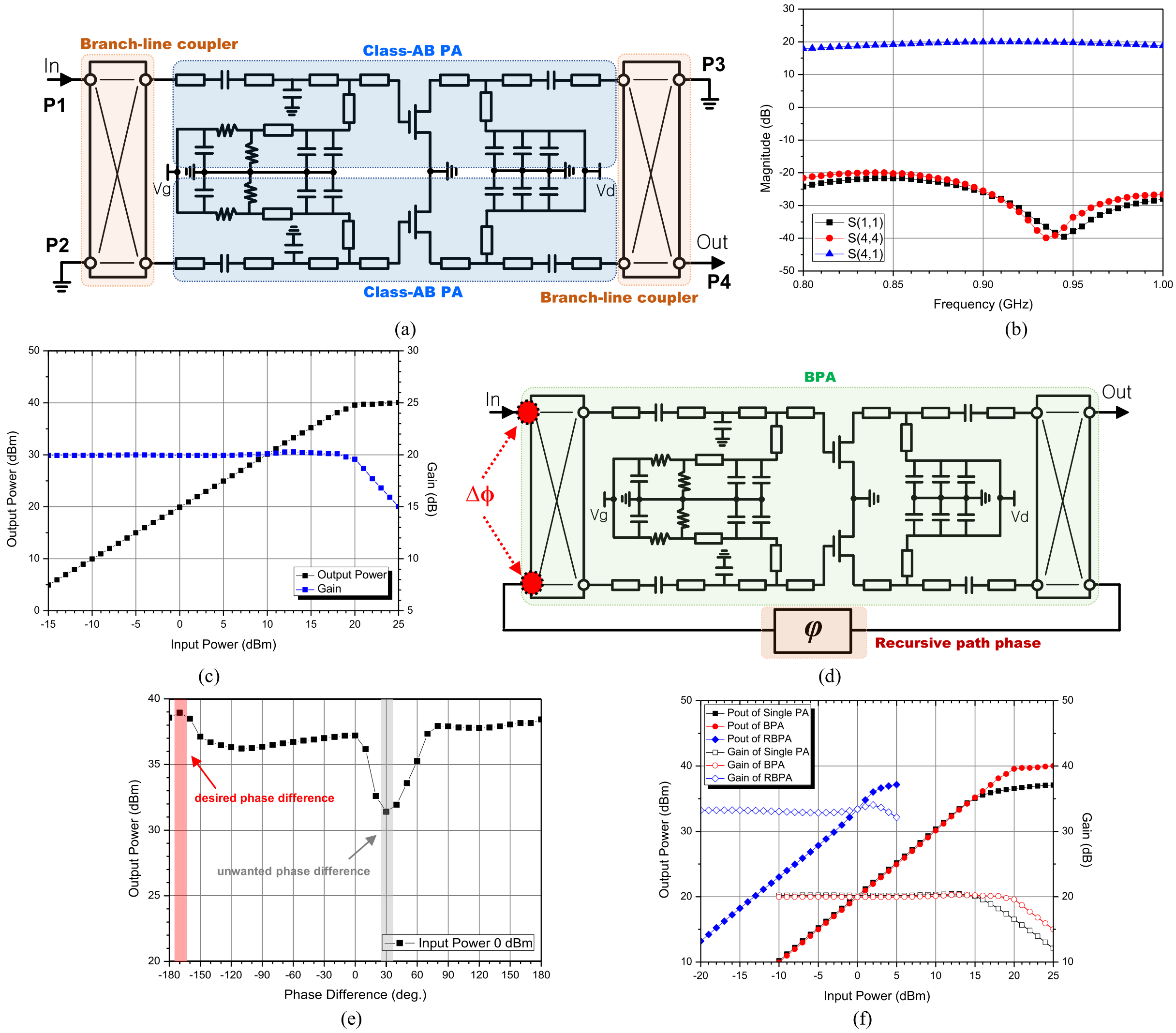


**FIGURE 5.** **Designed BPA with (a) circuit schematic, (b) simulated S-parameters, (c) simulated output power and gain, (d) recursive path with an arbitrary phase, (e) simulated output power according to the phase difference at IHC, and (f) overall comparison.**

with the insertion loss of 0.15 dB and the operation band from 815 to 960 MHz are adopted in this paper. Fig. 5 (a) shows the designed BPA and the simulated S-parameters are also shown in Fig. 5 (b). The simulated gain is similar to the single PA while the simulated bandwidth is widened due to the branch-line couplers. Also, Fig. 5 (c) shows the simulated output P1-dB of 39 dBm as theoretically expected. Then, the required feedback signal phase not to distract the input incoming signal is simulated for the BPA as shown in Fig. 5 (d). To ensure the recursive amplification, the recursive path phase is arbitrarily rotated and then optimized. The phase difference between the input port and the recursive path that makes the maximum output power near the saturation level is found as shown in Fig. 5 (e). Then, the simulated output powers and gains of the single PA, BPA and RBPA are compared in Fig. 5 (f). The RBPA shows the doubled maximum output power with the doubled gain, proving the feasibility for driverless high output power gain, proving the feasibility for driverless high output power generation.

As demonstrated in Fig. 5 (e), the optimized phase must be maintained in the feedback path to ensure the recursive operation. Thus, a reflection-type phase shifter (RTPS) is designed for the phase-controllable feedback network in this paper. Although many different types of phase shifters can be considered, the RTPS is chosen due to the advantages in design easiness, low-insertion loss, and continuous phase control [17]. Fig. 6 (a) shows the designed RTPS structure, where a circulator is used with a variable capacitor. By varying the load impedance through the variable capacitor, a signal can be reflected to the output port with a phase shift. Since the general discussion about the RTPS can be found in [17], the design steps are omitted in this paper. Fig. 6 (b) shows the simulated phase variation according to the variation in the capacitances of the RTPS. Since the phase shift shows the highest linearity from 0.1 to 2 pF capacitance range, the approximate phase variation range of 50° is expected in a practical design.

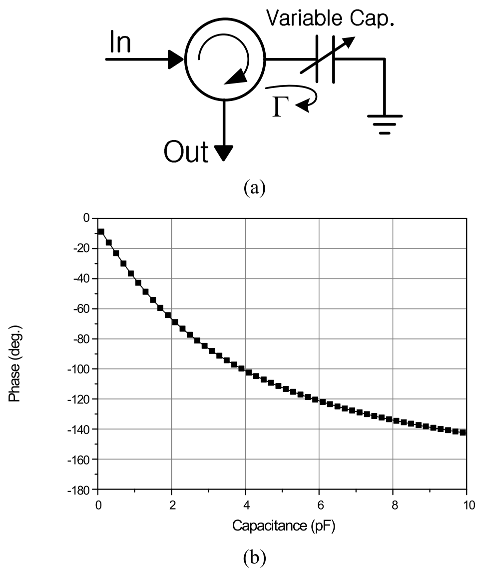


**FIGURE 6.** Circulator-based RTPS with (a) circuit schematic and (b) simulated phase shift according to capacitances.

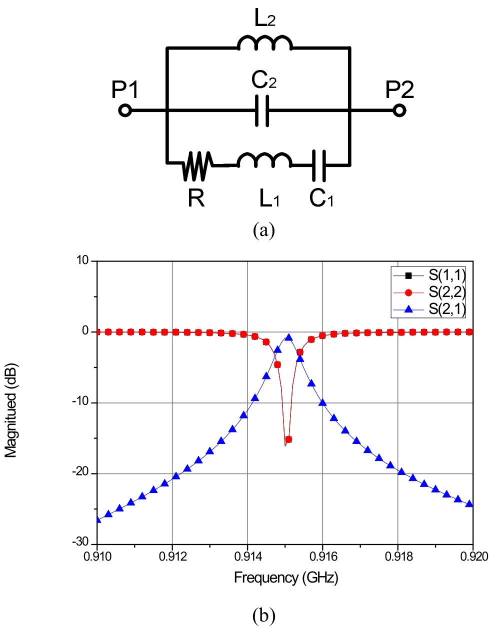


**FIGURE 7.** High-Q BPF with (a) equivalent lumped-circuit model and (b) simulated S-parameters.

To oscillate the RBPA at a desired center frequency, a high-Q BPF is further required in the feedback path. The BPF is designed with a commercially available SAW filter with an extra inductor connected in parallel in this paper. The equivalent lumped-circuit model is presented as shown in Fig. 7 (a), where R, $L_1$, $L_2$, $C_1$ and $C_2$ values are 9Ω, 25.2μH, 18.8 nH, 1.2 fF, and 1.6 pF, respectively. Fig. 7 (b) shows the simulated response, where the simulated Q-factor is about 1307, resulting in a high selectivity.

## III. FABRICATION AND MEASUREMENT

To implement the high power microwave signal generator, a single class-AB PA was first fabricated with the MW6S004NT1 power transistor and the conventional printed circuit board (PCB) process using a Teflon substrate as shown in Fig. 8 (a). The Teflon substrate has a relative permittivity of 2.54 and a thickness of 0.5 mm. Then, the fabricated PAs were connected in parallel by using LTCC hybrid couplers to form the BPA as shown in Fig. 8 (b). To compare the performance of the RBPA with the single PA and BPA, the phase controllable feedback network was also fabricated and connected with the BPA as shown in Fig. 8 (c). It is noted that the same Teflon substrate and PCB process were used for all circuit fabrication. Using the gate and drain voltages of 3.1 V and 28 V, respectively, the output power and gain characteristics were measured at 915 MHz as shown in Fig. 8 (d).

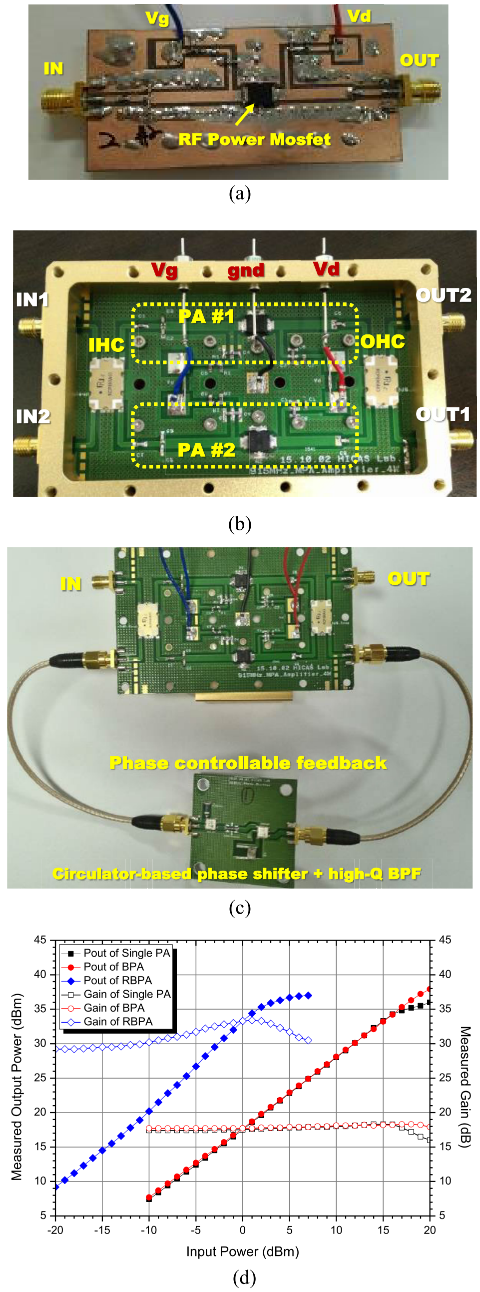


**FIGURE 8.** Implementation and measurement: (a) class AB single PA, (b) BPA (c) RBPA, and (c) output power and gain comparison.

**TABLE 1.** Comparison with previously reported feedback oscillators.

| Ref. | Feedback circuit | Freq. (GHz) | Output power (dBm) | Conv. efficiency (%) | Phase noise @ 100 kHz |
|---|---|---|---|---|---|
| [18] | BPF | 2.46 | 6.4 | 10 | -120.4 dBc/Hz |
| [19] | SRR | 1.98 | 9.5 | - | -127.2 dBc/Hz |
| [20] | SIW | 10.98 | -1.8 | - | -121.6 dBc/Hz |
| [21] | BPF | 8.2 | 4 | - | -140 dBc/Hz |
| This work | RMPA | 0.915 | 38.6 | 44.4 | -124 dBc/Hz |

The single PA shows the measured output P1-dB of 35.2 dBm with the gain of 17.2 dB while the BPA shows the measured output P1-dB estimation near 38.0 dBm with the approximate gain of 17 dB. It is noted that the exact output P1-dB of the BPA could not be obtained due to the limited output power of the signal generator used in this experiment. Lastly, the RBPA shows the output P1-dB of 38.4 dBm with the gain of 32 dB. Due to the balanced and recursive amplification, the measured output power and gain of the RBPA were increased by 3.2 dB and 14.8 dB from the single PA using the same RF power transistor.

Next, to verify the proposed high power microwave signal generation, the complete oscillator circuit was implemented with the RBPA, and the additional feedback networks as shown in Fig. 9 (a). One of the two feedback loops was connected through the sampling capacitor as described in Fig. 2 (a). Since the output power generated by the proposed oscillator was higher than the maximum allowable test power of the signal analyzer used in this experiment, a 30-dB fixed attenuator was used between the oscillator and the signal analyzer. Finally, to oscillate the complete circuit with the maximum output power, the recursive path phases were adjusted to the optimal phases, and the output power was measured at 915 MHz as shown in Fig. 9 (b). Since the output power of the proposed oscillator had been attenuated by 30 dB, the actual measured output power was calculated as 38.62 dBm. Since the total current of 585 mA was consumed with the supply voltage of 28 V to generate the output power of 38.62 dBm at 915 MHZ, the DC-to-RF conversion efficiency was measured as 44.43%. Furthermore, Fig. (c) shows the measured phase noise of −118.42 dBc/Hz at 10 kHz offset while the phase noise of −124 dBc/Hz was also measured at 100 kHz offset. Lastly, to compare the performance of the proposed RBPA-based signal generator with the other microwave feedback oscillators, a comparison table is summarized as follows.

The other feedback oscillators were configured by microstrip trisection BPF [18], split-ring resonator (SRR) [19], substrate integrated waveguide (SIW) bandpass response power divider [20], and elliptic filter with branch-line coupler [21] in the feedback circuitry. Since the phase noises of these oscillators were measured at 100 kHz offset or higher, the proposed oscillator phase noise was compared at 100 kHz offset instead of 10 kHz. Although some structures show lower phase noise, output power levels are also much lower while the proposed structure shows high output power with

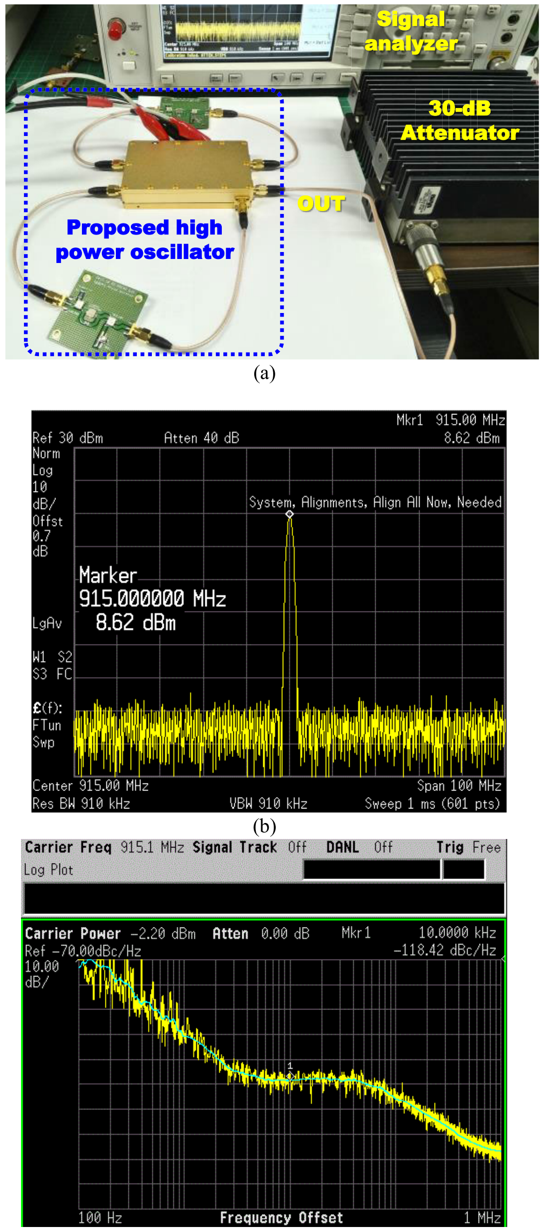


**FIGURE 9.** Proposed high power microwave signal generator with (a) implementation and test setup, (b) signal power measurement, and (c) phase noise measurement at 10 kHz offset.

high conversion efficiency and good phase noise. Therefore, the proposed structure can be an excellent candidate for high power oscillator satisfying both good phase noise and conversion efficiency.

## IV. CONCLUSION

The high-power microwave oscillator based on the RBPA, and phase controllable feedback networks was proposed in this paper. The signal from each output of the OHC continuously and alternately feedbacked to each input of the IHC, resulting in recursive amplification for high power generation. To verify the proposed high-power microwave oscillator, two LDMOS PAs in class-AB operation were first designed with the center frequency of 915 MHz. Then, the PAs were combined with two branch-line couplers operating as IHC and OHC to form a single BPA at 915 MHz. Next, the feedback circuits with the high-Q BPF and the phase shifter to control the recursive signal phase were designed and combined with the BPA to finally form the RBPA-based high-power microwave oscillator. With the supply voltage of 28 V, the proposed oscillator showed the measured output power of 38.62 dBm with the measured DC-to-RF conversion efficiency of 44.43% at 915 MHz. Also, the measured phase noises were −118 dBc/Hz and −124 dBc/Hz at 10 kHz and 100 kHz offsets, respectively.

## REFERENCES

[1] G. Gonzalez, *Foundations of Oscillator Circuit Design*. Norwood, MA, USA: Artech House, 2007.

[2] G. J. Linde, M. T. Ngo, B. G. Danly, W. J. Cheung, and V. Gregers-Hansen, "WARLOC: A high-power coherent 94 GHz radar," *IEEE Trans. Aerosp. Electron. Syst.*, vol. 44, no. 3, pp. 1102–1117, Jul. 2008.

[3] C. B. Barneto, T. Riihonen, M. Turunen, L. Anttila, M. Fleischer, K. Stadius, J. Ryynänen, and M. Valkama, "Full-duplex OFDM radar with LTE and 5G NR waveforms: Challenges, solutions, and measurements," *IEEE Trans. Microw. Theory Techn.*, vol. 67, no. 10, pp. 4042–4054, Oct. 2019.

[4] M. Kucharski, A. Ergintav, W. A. Ahmad, M. Krstic, H. J. Ng, and D. Kissinger, "A scalable 79-GHz radar platform based on single-channel transceivers," *IEEE Trans. Microw. Theory Techn.*, vol. 67, no. 9, pp. 3882–3896, Sep. 2019.

[5] S. Sancho, A. Suárez, F. Ramírez, and M. Pontón, "Analysis of the transient dynamics of microwave oscillators," *IEEE Trans. Microw. Theory Techn.*, vol. 67, no. 9, pp. 3562–3574, Sep. 2019.

[6] Y. Yuan, A. Y. Chen, and C. M. Wu, "Super-regenerative oscillator-based high-sensitivity radar architecture for motion sensing and vital sign detection," *IEEE Trans. Microw. Theory Techn.*, vol. 69, no. 3, pp. 1974–1984, Mar. 2021.

[7] M. Bahmanian and J. C. Scheytt, "A 2–20-GHz ultralow phase noise signal source using a microwave oscillator locked to a mode-locked laser," *IEEE Trans. Microw. Theory Techn.*, vol. 69, no. 3, pp. 1635–1645, Mar. 2021.

[8] W. Gerum, P. Malzahn, and K. Schneider, "94-GHz TWT for military radar applications," *IEEE Trans. Electron Devices*, vol. 48, no. 1, pp. 72–73, Jan. 2001.

[9] C. K. Chong and W. L. Menninger, "Latest advancements in high-power millimeter-wave helix TWTs," *IEEE Trans. Plasma Sci.*, vol. 38, no. 6, pp. 1227–1238, Jun. 2010.

[10] X. Chen, B. Yang, N. Shinohara, and C. Liu, "A high-efficiency microwave power combining system based on frequency-tuning injection-locked magnetrons," *IEEE Trans. Electron Devices*, vol. 67, no. 10, pp. 4447–4452, Oct. 2020.

[11] P. Livreri, "Design of a high-efficiency Ka-band TWT power amplifier for radar applications," *IEEE Trans. Plasma Sci.*, vol. 50, no. 9, pp. 2824–2829, Sep. 2022.

[12] G. K. Kornfeld, E. Bosch, W. Gerum, and G. Fleury, "60-GHz space TWT to address future market," *IEEE Trans. Electron Devices*, vol. 48, no. 1, pp. 68–71, Jan. 2001.

[13] M. L. Vecchi, F. Di Maggio, A. Spatola, R. Martorana, A. Mistretta, and P. Livreri, "Novel GaN based solid state power amplifiers, results, advances and comparison with vacuum tubes based microwave power modules," in *Proc. IEEE 4th Int. Forum Res. Technol. Soc. Ind. (RTSI)*, Sep. 2018, pp. 1–4.

[14] H. L. Lee, D.-H. Park, M.-Q. Lee, and J.-W. Yu, "Reconfigurable 2 × 2 multi-port amplifier using switching mode hybrid matrices," *IEEE Microw. Wireless Compon. Lett.*, vol. 24, no. 2, pp. 129–131, Feb. 2014.

[15] H. L. Lee, M. Lee, and J. Yu, "Reconfigurable 4 × 4 multi-port amplifier with switchable input and output matrices," *IET Microw., Antennas Propag.*, vol. 10, no. 12, pp. 1312–1321, Sep. 2016.

[16] H. L. Lee, M. Lee, and J. Yu, "Analysis of multi-port amplifier calibration for optimal magnitude and phase error detection," *IET Microw., Antennas Propag.*, vol. 10, no. 1, pp. 102–110, Jan. 2016.

[17] H. L. Lee, S.-M. Moon, M.-Q. Lee, and J.-W. Yu, "Design of compact broadband phase shifter with constant loss variation," *Microw. Opt. Technol. Lett.*, vol. 56, no. 2, pp. 394–400, Feb. 2014.

[18] C. Chang and C. Tseng, "Design of low phase-noise oscillator and voltage-controlled oscillator using microstrip trisection bandpass filter," *IEEE Microw. Wireless Compon. Lett.*, vol. 21, no. 11, pp. 622–624, Nov. 2011.

[19] Z. Cai, Y. Liu, X. Tang, and T. Zhang, "A novel low phase noise oscillator using stubs loaded nested split-ring resonator," *IEEE Microw. Wireless Compon. Lett.*, vol. 27, no. 4, pp. 386–388, Apr. 2017.

[20] R. Zhang, J. Zhou, Z. Yu, and B. Yang, "A low phase noise feedback oscillator based on SIW bandpass response power divider," *IEEE Microw. Wireless Compon. Lett.*, vol. 28, no. 2, pp. 153–155, Feb. 2018.

[21] H. Nimehvari Varcheh and P. Rezaei, "Low phase-noise X-band oscillator based on elliptic filter and branchline coupler," *IET Microw., Antennas Propag.*, vol. 13, no. 7, pp. 888–891, Jun. 2019.

**HAN LIM LEE** (Member, IEEE) received the B.A.Sc. degree in electronics engineering from Simon Fraser University, Burnaby, BC, Canada, in 2008, and the M.S. and Ph.D. degrees in electrical engineering from the Korea Advanced Institute of Science and Technology, Daejeon, South Korea, in 2010 and 2014, respectively. From 2014 to 2015, he was a Senior Engineer with the DMC Research Center, Samsung Electronics. In 2015, he joined the School of Electrical and Electronics Engineering, Chung-Ang University, Seoul, South Korea, where he is currently an Associate Professor. His research interests include microwave/RF circuits and communication systems, mmWave beamforming antennas and phased array systems, antenna-in-package (AiP), RFIC/MMIC, scalable-RF module, and microwave wireless power transmission (MWPT).

**SEUNG PYO PARK** received the B.S. and M.S. degrees in electrical engineering from the University of Seoul, Seoul, South Korea, in 2014 and 2016, respectively. In 2016, he joined Broadcom Inc., Seoul, where he is currently an Application Engineer. His research interests include wireless circuit and module applications. The contribution to this work was made during the M.S. degree pursuit.

**MOON-QUE LEE** (Member, IEEE) received the B.S. degree in electrical engineering from the Korea Advanced Institute of Technology, Daejeon, South Korea, in 1992, and the M.S. and Ph.D. degrees in electrical engineering from Seoul National University, Seoul, South Korea, in 1994 and 1999, respectively. From 1999 to 2002, he was a Research Engineer with the Electronics and Telecommunications Research Institute. Since 2002, he has been a Professor with the School of Electrical and Computer Engineering, University of Seoul, Seoul. Since 2015, he has been a Creative Planner for Radio & Satellite with the Ministry of Science, ICT and Future Planning, Korea Government. His research interests include microwave/millimeter wave circuits, monolithic microwave integrated circuits, hybrid circuits, wireless communication, and radar systems.